energy&fuels

pubs.acs.org/EF

Article

N-Vinyl Caprolactam/Maleic-Based Copolymers as Kinetic Hydrate Inhibitors: The Effect of Internal Hydrogen Bonding

Malcolm A. Kelland,* Janronel Pomicpic, Radhakanta Ghosh, and Safwat Abdel-Azeim

Cite This: *Energy Fuels* 2022, 36, 3088−3096

Read Online

ACCESS | Metrics & More | Article Recommendations

ABSTRACT: Kinetic hydrate inhibitors (KHIs) have been used for over 25 years to prevent gas hydrate formation in oil and gas production flow lines, but they are some of the most expensive oilfield production chemicals. The main component in KHI formulations is a water-soluble polymer with many amphiphilic groups. Usually, in commercial KHI polymers, the hydrophilic part of these groups is the amide group. In addition, KHI polymers are often incompatible with film-forming corrosion inhibitors. Therefore, we sought to find cheaper but effective KHIs that could also act as a flow line corrosion inhibitor. Continuing earlier work from our group with maleic-based polymers, we have now explored maleic acid/*N*-vinyl caprolactam (MAcid/VCap) copolymers to introduce VCap, a well-known KHI monomer, together with the cheaper MA monomer. KHI performance screening tests were conducted under high pressure with a structure II-forming natural gas mixture in steel rocking cells using the slow (1 °C/h) constant-cooling test method. Surprisingly, the MAcid/VCap copolymer showed very poor KHI efficacy. GFN2-xTB molecular dynamics simulations revealed that MAcid/VCap exhibits intra-hydrogen bond networks that trap the polymer morphology in the globular form. In this scenario, the caprolactam ring is encapsulated inside the polymer structure due to the intra-hydrogen bonds and the hydrophobic interactions that minimize its ability to interact with the hydrate surfaces, which significantly reduces the MAcid/VCap kinetic inhibition performance. However, the polymer in such globular forms still displays an important amount of its carboxylic groups exposed to water, which explains the water solubility. In contrast to MAcid/VCap copolymers, maleimide derivatives with dibutylamino end groups were effective KHIs and even better with dibutylamine oxide end groups. A terpolymer of MA/VCap reacted with *N*,*N*-dibutylaminopropylamine followed by subsequent oxidation of the end groups to dibutylamine oxide and gave the best performance of any maleic-based polymer reported to date. The combination of caprolactam and dibutylamine oxide groups can be thought of as synergism within the same polymer, akin to the excellent synergy of the separate molecules, tributylamine oxide and PVCap.

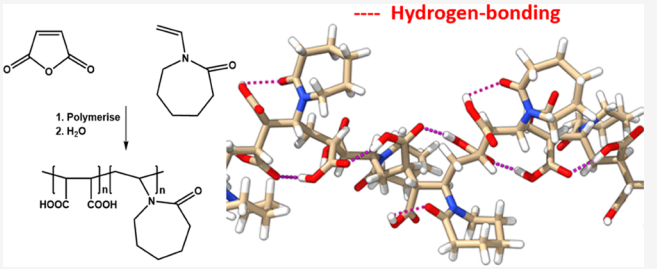

INTRODUCTION

Production of oil and gas has several flow assurance issues including corrosion and deposition of scale, wax, gas hydrates, and asphaltenes.[1,2] Chemicals can be used to combat each of these problems but usually each requires a different chemical. We have begun a program to develop multi-functional chemicals in an attempt to treat gas hydrates, corrosion, and scale, which are all water-based problems. Regarding the first issue, we have been designing and testing kinetic hydrate inhibitors (KHIs) as a method to prevent gas hydrate solids from forming in flow lines.[3−13] KHIs delay the hydrate formation process at the nucleation and crystal growth stages.[14,15] KHIs have been shown to both increase the nucleation work required to form critical nuclei and increase the effective number of sites where nucleation could occur.[16]

KHIs are formulations in which the main ingredient is one or more water-soluble polymers with amphiphilic functional groups. One of the most well-known classes of KHI polymers is *N*-vinyl caprolactam-based (VCap) polymers, several of which are deployed in the field. The homopolymer (PVCap) is often used as a standard for comparison to new KHI polymers and VCap/*N*-vinyl pyrrolidone (VCap/VP) copolymers, which have higher cloud points (Figure 1). However, caution must be taken in such a comparison because factors such as the polymer molecular weight distribution, method of polymerization, end-capping, and polymer solvent can affect the performance.[4,5]

Recently, we decided to focus on maleic-based polymers to develop a multi-functional chemical that could be tailored not only as a KHI but also for corrosion and scale inhibition. As far as we know, there are no polymers that function well in all three

Received: January 7, 2022
Revised: February 15, 2022
Published: February 23, 2022

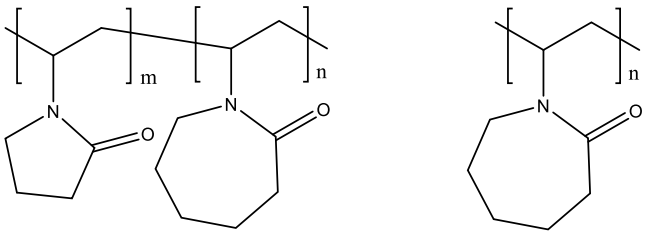

Figure 1. Left to right, *N*-vinyl pyrrolidone/*N*-vinyl caprolactam copolymer (VP/VCap) and poly(*N*-vinyl caprolactam) (PVCap).

ways, although there are KHIs with corrosion inhibition properties, corrosion inhibitors with scale inhibition properties, and scale inhibitors with KHI properties.[17−29] The reasoning was twofold. First, maleic anhydride (MA) is an abundant and cheap raw material. Second, polymers and copolymers of MA can be easily reacted with amine or alcohols to give a wide range of pendant functional groups connected to the polymer backbone.

Maleic-based KHI polymers have been known since the 1990's.[30] Improvements in KHI performance were recently reported for vinyl acetate/maleic anhydride (VA/MA) copolymers.[31] For example, reaction of the anhydride groups in the VA/MA 1:1 copolymer with a 60:40 mixture of cyclohexylamine:3-di-*n*-butylaminopropylamine (VA/MA-60%cHex-40% DBAPA, M_n = 11 kg/mol, 25 wt % in BGE) gave a significantly better performance than previously reported maleimide polymers (Figure 2) and no cloud point at 95 °C in water. This copolymer also showed good CO_2 corrosion inhibition properties.[32]

Another approach using maleic-based copolymers is to copolymerize MA with a known active KHI monomer such as VCap. This leaves the MA units free to be derivatized for incorporation of functional groups for corrosion and scale control. Here, we present work carried out on MA/VCap and MA/*N*-vinyl pyrrolidone (MA/VP) copolymers and their use as starting materials to a range of other copolymers that have been screened for KHI performance. Excellent KHI performance was obtained for the best polymers, better than all previously reported MA-based KHI polymers. This work is the foundation for development of our MA/VCap-based multi-functional hydrate-scale corrosion inhibitors, which we will report on in later publications.

EXPERIMENTAL SECTION

Materials. MA (≥99%), xylene (99%), 1,2-dimethoxyethane (DME, 99%), 2-butoxyethanol (BGE, 99%), hydrogen peroxide (30 wt % in water), azobisisobutyronitrile (AIBN), iso-butylamine ($iBuNH_2$), *n*-butylamine ($nBuNH_2$), cyclohexylamine ($CyHexNH_2$), n-1-butylpiperazine (nBuPiperazine), and 3-(dibutylamino)-1-propylamine (DBAPA) were purchased from VWR (Avantor) and used as received. Poly(*N*-vinyl caprolactam) (PVCap) (Mw approximately 2−4 kg/mol) was supplied by BASF as Luvicap EG, a 41.1 wt.% solution of the polymer in monoethylene glycol. The solvent was removed for this study by repeated precipitation of the polymer from aqueous solution above the cloud and deposition point (ca. 40 °C). Synthesis of polymaleic anhydrides was carried out according to the literature,

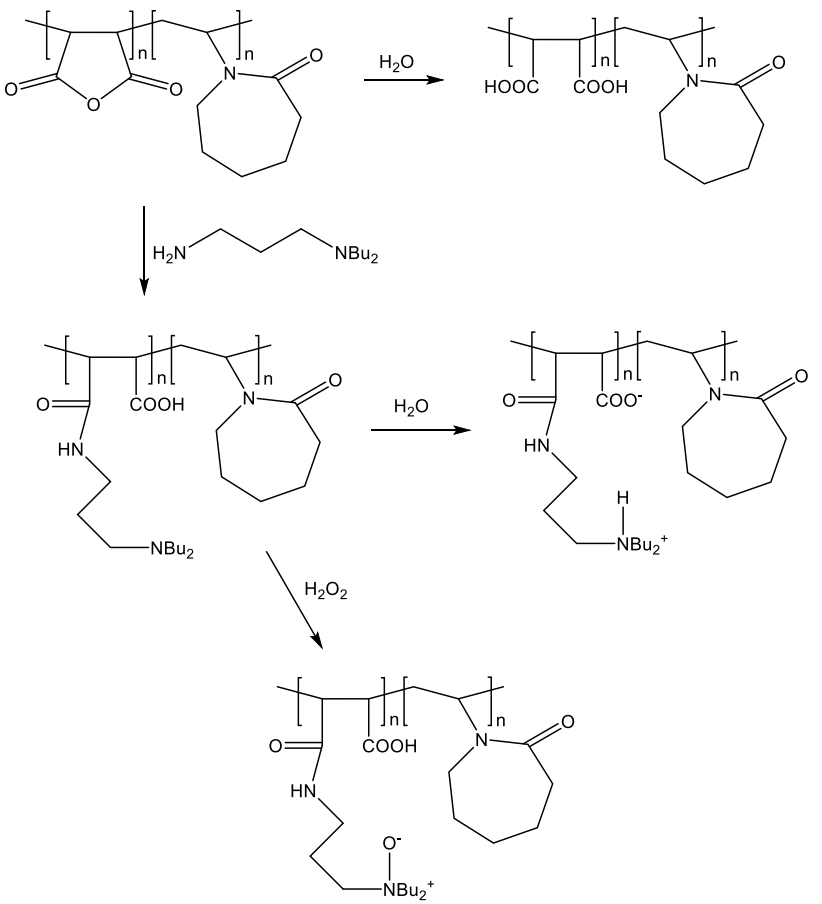

Figure 2. Reaction of the MA/Cap copolymer with either water or with DBAPA and subsequent formation of the amine oxide polymer (MA/VCap-DBAPA-AO).

https://doi.org/10.1021/acs.energyfuels.2c00075
Energy Fuels 2022, 36, 3088−3096

except that toluene was replaced with xylene or DME.[31] Polymer molecular weight analysis for all polymers was carried out by GPC/SEC using DMF solvent at 0.6 mL/min, 40 °C, using polystyrene standards.

Polymer Synthesis. MA/VCap and MA/VP copolymers were made in the same way using the AIBN initiator and either xylene or DME as solvent. Solvent was removed to leave a solid copolymer, which was always stored in an air-tight container before further use. It is important to keep MA-based polymers dry before reacting with amines or alcohols or else water vapor opens the anhydride ring to give two carboxylic acids groups, neither of which will react easily with the amines or alcohols under the conditions used. Examples of the three synthesis procedures in this study are given here: they include an example of copolymer MA:*N*-vinyl lactam synthesis, its reaction to open the ring of the MA group with a primary amine [the example given is for *N*,*N*-dibutylaminopropylamine (DBAPA)], and reaction of tertiary amine groups in a polymer with hydrogen peroxide to make amine oxide groups (Figure 2).

Synthesis of poly(maleic anhydride-*co*-*N*-vinylcaprolactam). Maleic anhydride (2.45 g and 0.025 mol) was first weighed in a round-bottom flask. Afterward, AIBN (0.41 g and 0.0025 mol), *N*-vinylcaprolactam (3.48 g and 0.025 mol), and then 50 mL of DME were added. The air was then removed, and then, a stream of N_2 gas was flushed into the flask. The system was then heated at a temperature of 70 °C and stirred for 15 h. After the reaction, the system was then cooled, and the solvent was decanted and removed via rotary evaporation to obtain the resulting product, alternating MA/VCap 1:1 copolymer.

Reaction of poly(maleic anhydride-*co*-*N*-vinylcaprolactam) with DBAPA. Poly(maleic anhydride-*co*-*N*-vinylcaprolactam) (0.174 g) was weighed in a vial, and DBAPA (0.137 g and 0.00074 mol) and BGE solvent (0.894 g and 0.0076 mol) were added. The mixture was stirred at room temperature for 16 h until complete dissolution to give a 25.8 wt % solution of the MA/VCap-DBAPA polymer with one DBAPA attached per MA monomer unit (Figure 2).

Synthesis of MA/VCap-DBAPA-AO. 0.311 g of DBAPA-modified poly(maleic anhydride-*co*-*N*-vinylcaprolactam) (MA/VCap-DBAPA) was reacted with 0.083 g of a 30 wt % solution of hydrogen peroxide. The solution was then stirred for 16 h at room temperature to give the amine oxide MA/VCap-DBAPA-AO with one DBAPA-AO attached per MA monomer unit (Figure 2).

Cloud Point (T_{Cl}) Measurement. A 2500 ppm aqueous solution of the polymer was heated slowly. The temperature at the first sign of clouding of the solution was taken as the cloud point. Any solution that was already opaque or cloudy at room temperature was first kept in a cooling room at 4 °C before heating. Cloud point measurements were repeated three times to check reproducibility.

KHI Experimental Test Procedure. A multi-stainless-steel rocker rig supplied by PSL Systemtechnik, Germany, and Svafas, Norway, was used to conduct KHI performance tests. This apparatus can rock five 40 mL cells in a cooling bath, with each cell equipped with temperature and pressure sensors. A stainless-steel ball is placed in each cell for agitating the test solution during rocking. A synthetic natural gas mixture (SNG, Table 1) was used, which preferentially forms structure II gas hydrates as the most thermodynamically stable phase.

KHIs were evaluated for performance by the slow constant-cooling (SCC) experimental method, which is summarized as follows:[32]

1. Test chemicals were dissolved to the desired concentration in deionized water (DIW) usually 1 day in advance of the test.
2. 20 mL of test solution was added to each of the five cells.
3. Using repeated vacuum and pressurizing with SNG, the air in the cells was replaced with SNG up to 76 bar.
4. The cells were rocked at a rate of 20 rocks per minute with an angle of 40°, while being cooled at 1.0 °C/h from 20.5 to 2.0 °C.

By standard laboratory dissociation experiments, the hydrate equilibrium temperature (T_{eq}) at 76 bar was determined to be 20.2 ± 0.05 °C warming at 0.025 °C/h for the last 3−4 °C, which correlates well with calculations performed using Calsep PVTSim software.[33] During a SCC experiment, there is a linear pressure decrease from which both the onset temperature for hydrate formation (T_o) and the rapid hydrate formation temperature (T_a) can be observed (Figure 3). In the example shown, T_o is 11.2 °C and T_a is 10.0 °C. Each cell is a closed system. From this linear pressure decrease, the temperature at the first observable deviation is defined as T_o. This is the first macroscopic observation of hydrate formation carried out by an observation on a linear pressure decrease, and therefore, it is quite possible that the hydrate nucleation is initiated at a molecular level prior to this. These experiments, however, may not be capable of detecting the start of nucleation, which possibly happens earlier than T_o. T_a is taken as the temperature when the pressure decrease is the steepest, that is, when the hydrate formation is the fastest. The standard deviation (assuming a normal distribution) for a set of T_o or T_a values is no more than 0.6 °C and usually less than 0.3 °C. The scattering still allows for a rough ranking of the performance of the KHI samples as long as sufficient tests are carried out for a statistically significant difference using a *t*-test. Depending on the variation in average T_o between samples, 5−10 tests suffices in most cases to get a significant difference at the 95% confidence level ($p < 0.05$).[34]

Modeling Work: GFN2-xTB Molecular Dynamics Simulations on the MAcid/VCap 1:1 Copolymer. Molecular dynamics (MD) simulations are performed on alternating MAcid/VCap 1:1 oligomers of 40-mer lengths in order to examine the polymer conformational changes that probably would impact its interactions with the hydrate surfaces. The GFN2-xTB method[35] with the extended tight-binding Hamiltonian[36,37] was used to sample the polymer chain conformation due to its efficiency. GFN2-xTB is a semi-empirical quantum method based on density functional tight-binding theory developed by Grimme's group. The method has primarily targeted the computation of properties around the energy minima such as **g**eometries, vibrational **f**requencies, and **n**on-covalent interaction energies. The **GFN** refers to the calculated properties, and **xTB** stands for the extended tight-binding Hamiltonian. There are three variants of GFNn-xTB that are developed (n = 0, 1, and 2), which differ in accuracy and efficiency. They have been successfully applied in the optimization of organo-metallic complexes, structure sampling, exploring the reaction profiles, and macromolecule structure optimization.[38−48] In addition, the electronic effects are still included at the semiempirical level of theory, which are challenging systems for the DFT method.[49] The empirical FF parameters for the GFN2-xTB method are fitted to reproduce the results of DFT (B97-3c).[50] Prior to MD production, an energy minimization step is performed to remove the bad atomic contacts in the initial polymer coordinates. MD simulations were conducted for 1 ns at 278 and 300 K using the XTB code[51] and in an implicit water environment using the analytical linearized Poisson-Boltzmann (ALPB) model.[52,53] The implicit solvent model was chosen to minimize the computational cost; such a system is not affordable in an explicit water environment (702 atoms). Furthermore, ALPB models the interactions with the solvent molecules accurately by including polar and non-polar contributions and correction for hydrogen bonding interaction. Such treatment demonstrates very accurate performance in predicting the geometries, binding energies, hydration free energies, and the octanol−water partition coefficient compared to their experimental counterparts.[52] Furthermore, details on the GFN2-xTB method and its applications have been published.[54]

The MAcid/VCap 1:1 polymer (Figure 4) was considered for our MD simulations as the remaining polymers in this study do not display the capacity to form intra-HBs. Concerning the MAcid/VP 1:1

Table 1. Composition of the SNG Mixture Used in the Performance Testing

component	mol %
nitrogen	0.11
n-butane	0.72
isobutane	1.65
propane	5.00
CO_2	1.82
ethane	10.3
methane	80.4

https://doi.org/10.1021/acs.energyfuels.2c00075
Energy Fuels 2022, 36, 3088−3096

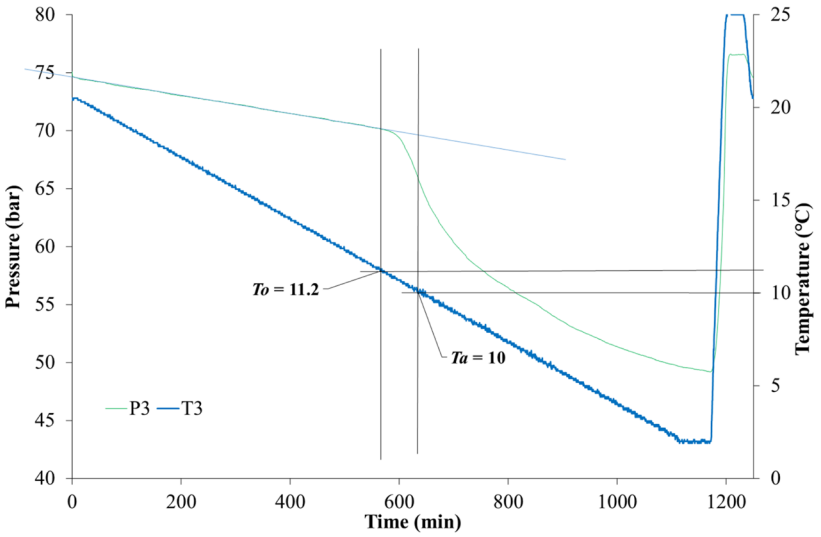

Figure 3. Determination of T_o and T_a values for one rocking cell experiment.

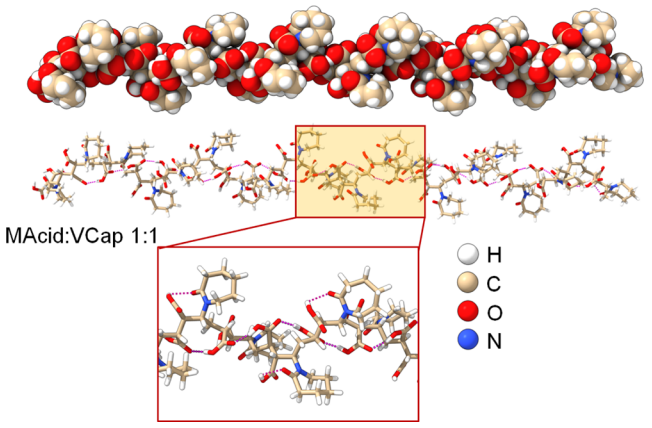

Figure 4. Optimized structure of the MAcid/VCap copolymer is represented in spheres and sticks, showing the intra-hydrogen bonds (HBs) along the polymer backbone. Optimization was carried out in an implicit solvent environment (no explicit water molecules are considered).

copolymer, it has the same capacity to form intra-HBs, and we focused on MAcid/VCap 1:1 due to the computational cost.

RESULTS AND DISCUSSION

Experimental Study of Kinetic Gas Hydrate Inhibition.

Table 2 summarizes the SCC results with all polymers in this study. DIW, and PVCap were also tested for comparison. A concentration of 2500 ppm (0.25 wt %) was chosen as a typical field dosage. We chose to use T_o values to evaluate the performance of a KHI as total inhibition of detectable hydrate formation is preferred for avoiding any chance of deposits building up in flow lines. $T_o - T_a$ values can give some indication of the ability to slow the growth of hydrate crystal formation although caution must be taken. Comparisons are only valid if T_o values are similar as the driving force when crystal growth occurs ought to be similar. In Table 2, $T_o - T_a$ values for maleic polymers are quite low (<1 °C), indicating that these polymers are not good at preventing macroscopic crystal growth.

We prepared MA-based polymers (PMA, MA/VCap copolymer, and MA/VP copolymer) in both xylene and DME to investigate the difference between solvent polarity. Not all

Table 2. Summary of Slow Constant-Cooling KHI Test Results. All Solutions Were Clear Unless Otherwise Stated

	polymer name	molecular weight, M_n (g/mol)	T_o (av.) [°C]	T_a (av.) [°C]
1	no additive		16.0	15.7
2	PVCap		9.8	9.4
	maleic polymers made in DME			
3	MAcid/VCap-1	15 500 (PDI 2.85)	14.2	13.9
4	MA/VCap-1-DBAPA[a]	25 700	5.6	5.4
5	MA/VCap-1-CyHexNH$_2$[a]	20 428	8.6	8.4
6	MA/VCap-1-nBuNH$_2$[a]	18 847	7.3	7.2
7	MA/VCap-1-iBuNH$_2$[a]	18 847	7.2	7.0
8	MA/VCap-2′	10 000		
9	MA/VCap-2-DBAPA[a]	16 594	5.6	5.4
10	MA/VCap-2-DBAPA-AO[a]	17 299	3.9	3.7
11	MA/VCap-2-nBuPiperazine[a]	14 866	8.7	8.6
12	MA/VCap-2-nBuPiperazine-AO[a]	15 571	8.5	8.2
	repeat with new polymer batch[a]	15 571	9.0	8.7
13	MAcid/VP	35 500 (PDI 3.34)	15.5	14.9
14	MA/VP-DBAPA[a]	61 800	8.4	7.6
15	MA:VP-DBAPA-AO[a]	64 612	7.7	7.0
	maleic polymers made in xylene			
16	PMAcid	800 (PDI 3.8)	16.1	15.9
17	MAcid/VCap-3[a]	9800 (PDI 3.69)	14.8	14.5
18	MA/VCap-3-DBAPA[a]	16 262	6.0	5.4
19	MA/VCap-3-CyHexNH$_2$[a]	48 180	9.3	9.0
20	MA/VP-DBAPA-AO[a]	64 633	8.6	7.7

[a]25-58 wt % solution in BGE.

polymers were made in both solvents but sufficient to show that there was not much difference between the use of the two solvents (Table 2). We preferred DME as solvent as it was easier to remove after polymerization by rotary evaporation and vacuum-drying.

As discussed in the introduction, MA/VCap and MA/VP copolymers have previously been shown to be alternating ABABAB copolymers.[55−58] Table 2 gives the molecular weights of the hydrolyzed versions of these copolymers (MAcid versions) from GPC analysis and for the PMAcid homopolymer.

https://doi.org/10.1021/acs.energyfuels.2c00075
Energy Fuels 2022, 36, 3088−3096

Reaction of the MA copolymers with 1 equivalent of amine per MA unit went to completion as judged by 1H NMR spectroscopy and as previously reported.[30,59] This means that there was one amine attached per MA unit (Figure 2). Therefore, the molecular weights of the aminated copolymers can be determined by adding the molecular weights of the MA/VCap or MA/VP copolymers and the amines. These values are given in Table 2.

Considering the good performance of PVCap and many previously investigated VCap copolymers, we were initially very surprised to find that MA/VCap when hydrolyzed to the maleic acid/VCap copolymer (MAcid/VCap) gave very poor performance as a KHI. The average T_o values for the MAcid/VCap copolymers made in DME and xylene were 14.2 and 14.8 °C, respectively (Entries 3 and 17 in Table 2), not much better than no additive or PMA homopolymer (Entries 1 and 16). The same poor performance was also seen for the MAcid/VP copolymer (entry 13). MA/VCap-2 (entry 8) was not tested as a KHI as it was clear that it would not perform well due to the poor performance of MAcid/VCap-1 (entry 3). Instead, it was directly derivatized with amines (Entries 9−12).

We wondered what the reason was for the poor performance of the MAcid:*N*-vinyl lactam 1:1 copolymers. First, we noted that MA polymerizes poorly by itself but forms alternating ABABAB copolymers with a number of comonomers if the molar feed ratio is 1:1.[55] This has been reported for the MAcid/VP 1:1 copolymer.[56] A kinetic investigation by proton nuclear magnetic resonance spectroscopy (^{1}H NMR) showed that both monomers had identical polymerization rates if both monomers were present in the reaction mixture.[57] The MAcid/VCap 1:1 copolymer has also been reported to have a high amount of alternating copolymers.[58] This study also showed by FTIR spectroscopy at various pH values that this copolymer has considerable internal hydrogen bonding between the maleic acid and VCap units, which obviously is not present in PVCap (Figure 5).

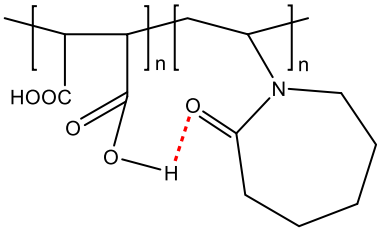

Figure 5. Crude sketch of the possible internal hydrogen bonding for the MAcid/VCap copolymer.

From the above studies, we assume that our MA/VCap will also be a highly alternating ABAB copolymers. We also wondered if the internal H bonds were the reason for the poor KHI performance. This might cause the polymer to curl up on itself, which would hide a large part of the polymer from interacting with water or hydrate surfaces. At the same time, the copolymer does not lose water solubility due to the second carboxylic acid group on each maleic unit, which is free to interact with water. We carried out computer modeling studies to help probe this theory. These are discussed in the next section.

Compared to MAcid/VCap, derivative copolymers made by reacting MA/VCap with amines all gave improved KHI performance (Table 2). These amide-forming reactions were performed in BGE solvent, which is a known synergist for PVCap and other polyamide-based KHI polymers.[60−63] PVCap, with a similar amount of added BGE, was shown to give an average T_o of 7.3 °C under the same test conditions in the same rocking cell apparatus.[64]

Of the various amines used, DBAPA clearly gave the best performance, giving average T_o value, at least 1.5 °C better than all the other amines used. The other amines, *n*-butylamine, isobutylamine, cyclohexylamine, and butylpiperazine, were chosen based on previous maleic-based KHI polymer studies. Entries 4 and 9 in Table 2 give results for two different-molecular weight MA/VCap-DBAPA copolymers for which the initial MA/VCap was made in DME. Entry 18 gives the results for a third MA/VCap-DBAPA copolymer for which the precursor MA/VCap was made in xylene. All three copolymers have fairly similar results, with no statistically significant difference, with average T_o values between 5.6 and 6.0 °C, better than PVCap with a similar concentration of added BGE. To compare the KHI performance of two polymers, it is important that they have the same functional groups and similar molecular weight in order to get a valid comparison. The MAcid/VCap-3 (entry 17) made in xylene has M_n 9800 g/mol, which is similar to MAcid/VCap-2 made in DME with M_n 10 000 g/mol (entry 8). Therefore, derivatives of these two copolymers can be compared. We can then see that MA/VCap-2-DBAPA has average T_o = 5.6 °C and MA/VCap-3-DBPAP has average T_o = 6.0 °C. These values are too close to be able to claim that one polymer is better than another.

The dibutylamino end groups may be partially quaternized due to self-ionization in water as shown in Figure 6. These

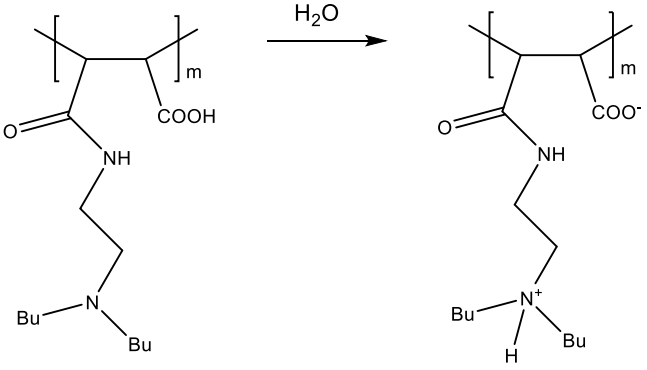

Figure 6. Self-ionization of MA-DBAPA monomer units.

dibutylammonium groups may contribute to give improved performance as seen in other polycationic KHIs and synergistic mixtures of quaternary ammonium salts and VCap-based polymers.[65−69]

We knew from past studies that oxidizing the dibutylamino group to dibutylamine oxide could improve the performance for other polymer classes.[31,32] Therefore, we first reacted MA/VCap-DBAPA with hydrogen peroxide to form MA/VCap-DBAPA-AO (entry 10, Table 2). The performance increased substantially as observed from the average T_o value dropping by a statistically significant 1.7−3.9 °C compared to the parent polyamine (entry 9, T_o = 5.6 °C) ($p < 0.05$ in a *t*-test). This is an excellent T_o value, better than any other reported maleic-based KHI polymer. Butylated amine oxides are known to be good synergists for VCap-based polymers, so the improved performance result for MA/VCap-DBAPA-AO could be construed as an internal synergy.[70] In contrast, MA/VP-DBAPA-AO (Entries 15

https://doi.org/10.1021/acs.energyfuels.2c00075
Energy Fuels 2022, 36, 3088−3096

and 20) did not exhibit such a strong performance increase as observed for the equivalent VCap copolymer. The MA/VP-DBAPA-AO polymer made in DME gave a statistically significantly lower average T_o value by 0.9 °C than the same polymer made in xylene. The lower performance of the MA/VP-based copolymer compared to the MA/VCap polymer performance fits with the known poorer performance of PVP compared to PVCap performance.[3,5,6,9] Finally, we also made MA/VCap-2-nBuPiperazine-AO, the amine oxide of MA/VCap-2-nBuPiperazine (entry 12). This polymer did not show an improvement over the piperazine precursor, possibly because there is only one pendant butyl group compared to two butyl groups in MA/VCap-DBAPA-AO.

Solutions of KHI polymers in produced water can be subjected to elevated temperatures both at the well head and during processing. Above the cloud point temperature, the polymer could precipitate and cause deposits. Therefore, a high cloud point in the produced water is a useful property although it can often give lower KHI performance than a more hydrophilic polymer in the same class.[2,71] The cloud point of the most effective KHI polymer MA/VCap-DBAPA-AO was determined at various salinity values using a 2500 ppm solution of the polymer. The results are given in Figure 7. In DIW, the cloud

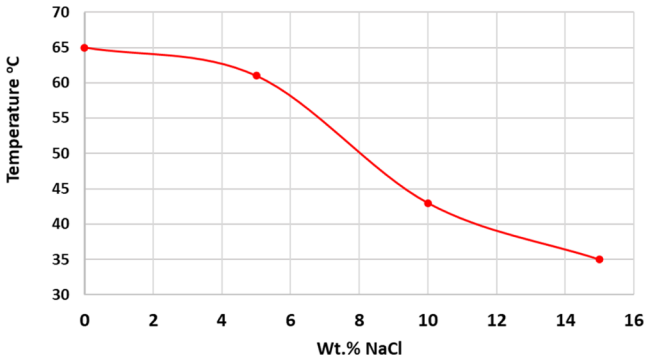

Figure 7. Cloud point of 2500 ppm solution of MA/VCap-DBAPA-AO at various salinity values.

point was 65 and decreased to 35 °C in 15 wt % NaCl. For the more hydrophilic polymer MA:VP-DBAPA-AO, there was no cloud point even in 15 wt % NaCl, giving this polymer an excellent compatibility temperature range even with high salinity brines. We will report on the KHI efficacy of these polymers in high salinity brines in later work.

Molecular Dynamics Simulations. GF2-xTB MD simulations were carried out on the MAcid/VCap copolymer in order to examine the impact of its intra-HB network on the polymer morphology in an implicit water phase. We have simulated the polymer at two different temperatures: 300 and 278 K; the latter is the operational temperature. We also examined the effect of the pH on the protonation state of its carboxylic groups (low pH = 3.5). The repeating unit of MAcid that carries the carboxylic groups is succinic acid; its pK_a values are 4.21 and 5.64,[72] which means that at pH 3.50, most carboxylic groups (83.9%) are in the protonated state.[73] Popescu et al. reported even lower pK_a values in the presence of 0.02 N $CaCl_2$ (3.5 and 6.1).[74] Therefore, we modeled the MAcid/VCap copolymer with 20% of its carboxylic groups in their deprotonated state (i.e., dissociated form).

The radius of gyration (R_g) is a key parameter usually used to monitor the conformational changes of the macromolecules.[75−77] Figure 8 depicts the time evolution of R_g of MAcid/VCap under different conditions of temperature and

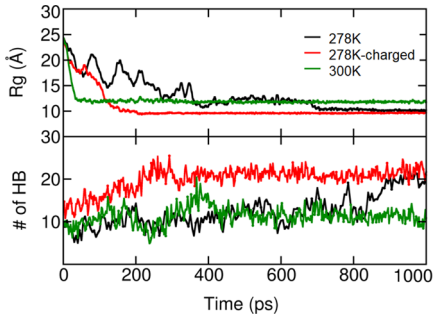

Figure 8. Time evolution of the internal HBs and radius of gyration (Rg) of the MAcid/VCap polymer simulated at 278 and 300 K.

total charge. MD of MAcid/VCap at different temperatures and in different charged states simulated for 1 ns revealed a compact morphology that curled up to form a globular structure. R_g of MAcid/VCap changes from 24 to 10.0 Å at 278 K and to 11.6 Å at 300 K. At low temperature (278 K), the polymer loses almost 60% of its hydrodynamic size and 50% of its hydrodynamic size at room temperature (300 K). The polymer is transformed into the same globular conformation (Figures 8 and 9), irrespective of its charged state (i.e., the carboxylic groups are fully undissociated or partially dissociated). In its neutral and charged states, the polymer displayed the same intra-HBs during the last 100 ps. However, the charged state quickly adopts the compact conformations mainly because of its higher density of intra-HBs than the neutral state (Figure 9). The presence of some carboxylate anions along the polymer backbone drives the conformational transition into the globular form faster than the polymer with fully undissociated carboxylic groups. The dissociated carboxylic group establishes strong HBs with the amide group of VCap and the second undissociated carboxylic group.

The neutral state simulated at 278 K exhibits conformational fluctuations in the early dynamics; however, it gets compacted after 400 ps and is trapped into even more compact structures during the last 300 ps. At such low temperatures, the polymer backbone dynamics are slow, and it is easily trapped into shallow minima, which slows down its transition to the globular form compared to the charged state. At 300 K, the polymer changes into the compact conformation even before the first 50 ps. Still, it displays a more extended structure than at 278 K (Figures 8 and 9d) because at a higher temperature, the polymer backbone can overcome the shallow energy barriers and sample more extended structures. The intra-HB network is established between the carboxylic groups with themselves and with the Cap group (Figure 9e). The conformational transition observed in our simulation is in very good agreement with what is reported in the literature of the MAcid/VCap viscosity reduction at pH = 3.5.[74] Indeed, at this pH, the authors noted that the solution becomes turbid, and the reduced viscosity is zero. Due to the high density of the intra-HBs, the polymer aggregates and undergoes a significant hydrodynamics size reduction, which is evidenced in our MD simulation.

The Cap is encapsulated inside the polymer structure in the globular form due to the intra-HBs and the van Der Waals interactions. In this scenario, the Cap does not have access to interact with the hydrate surfaces, which significantly degrades

https://doi.org/10.1021/acs.energyfuels.2c00075
Energy Fuels 2022, 36, 3088−3096

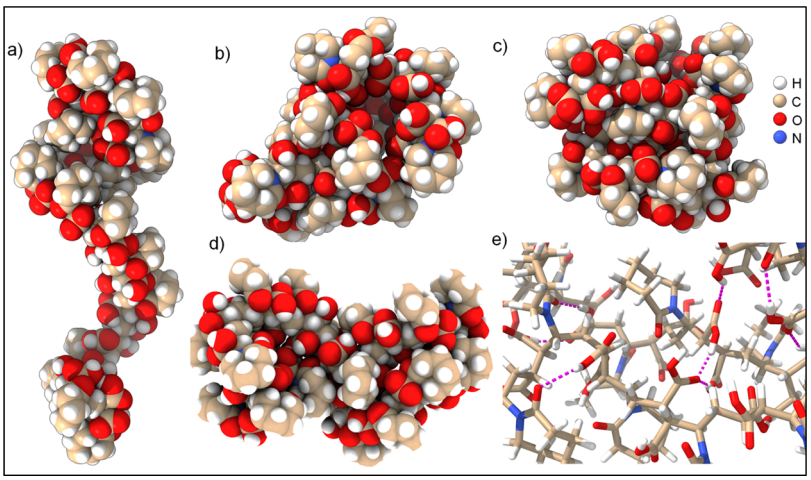

Figure 9. Structures of the MAcid/VCap copolymer at different temperatures and in different charged states. (a) Snapshot of an intermediate state of MAcid/VCap simulated at 278 K with zero total charge (time = 160 ps), (b,c) final morphologies of MAcid/VCap with zero and four total negative charges, respectively. (d,e)Final morphology simulated at 300 K, and zero total charge is shown in spheres and sticks with the intra-HBs shown by dashed lines.

the MAcid/VCap inhibition performance. The polymer is indeed trapped in the globular form; however, it still displays an essential amount of its carboxylic groups exposed to water that explains the reservation of its solubility. The latter is in good agreement with the dynamic light scattering results at different pH values; at pH = 5, the hydrodynamic diameter of MAcid/VCap is about 300 nm, while at pH = 3.9, it is 80 nm. Therefore, at low pH, the polymer forms small globular nanoparticles, and they are dispersed in water.

CONCLUSIONS

Low-molecular weight copolymers of MA/VCap or MA/VP were made in DME or xylene. Dissolution in water gave MAcid/VCap and MA/VP copolymers. Both were found to give very poor KHI performance in SCC screening tests in steel rocking cells using 76 bar SNG. The surprisingly poor performance was investigated using molecular dynamics simulations. These were performed at the GFN2-xTB level of theory, highlighting the role of the intra-HB networks in trapping the polymer morphology in the globular form rather than in the coil one. In such morphology, the Cap units are encapsulated and protected from the interactions with the hydrate surfaces. The MD simulations revealed that the origin of these intra-HBs are not limited to those formed between the MAcid carboxylic and the amide of the Cap units but between the MAcid carboxylic groups themselves at different distances along the polymer backbone. We also observed an important role of a small fraction of dissociated carboxylic groups that accelerates the polymer coil−globular transition.

Reaction of MA/VCap with various amines removed the internal H bonding and gave much improved KHI performance. The best amine derivative of MA/VCap was MA-VCap-DBAPA, but the performance was improved further by converting the dibutylamino end groups to dibutylamine oxide groups. This we have termed internal synergism within the copolymer, akin to the excellent external synergy of separate molecules such as tributylamine oxide and PVCap. The performance of MA:VCap-DBAPA-AO is the best we have seen reported for any maleic-based polymer. The addition of BGE solvent is also helpful for further KHI performance enhancement. We are now designing derivatives of MA/VCap and MA/VP copolymers for multi-functionality such as KHIs, CIs, and SIs. The DBAPA amine oxide group is a key feature in these studies.

AUTHOR INFORMATION

Corresponding Author

Malcolm A. Kelland − *Department of Chemistry, Bioscience and Environmental Engineering, Faculty of Science and Technology, University of Stavanger, Stavanger N-4036, Norway;* orcid.org/0000-0003-2295-5804; Email: malcolm.kelland@uis.no

Authors

Janronel Pomicpic − *Department of Chemistry, Bioscience and Environmental Engineering, Faculty of Science and Technology, University of Stavanger, Stavanger N-4036, Norway*

Radhakanta Ghosh − *Department of Chemistry, Bioscience and Environmental Engineering, Faculty of Science and Technology, University of Stavanger, Stavanger N-4036, Norway*

Safwat Abdel-Azeim − *Center of Integrative Petroleum Research (CIPR), College of Petroleum and Geosciences (CPG), King Fahd University of Petroleum and Minerals, Dhahran 31261, Saudi Arabia;* orcid.org/0000-0001-8611-1251

Complete contact information is available at: https://pubs.acs.org/10.1021/acs.energyfuels.2c00075

Notes

The authors declare no competing financial interest.

ACKNOWLEDGMENTS

We thank the Research Council of Norway (project no. 308813) for financial support of this work.

REFERENCES

(1) Frenier, W. F.; Ziauddin, M. *Chemistry for Enhancing the Production of Oil and Gas*; SPE Books, 2014.

(2) Kelland, M. A. *Production Chemicals for the Oil and Gas Industry*, 2nd ed.; CRC Press: Boca Raton, FL, 2014.

(3) Sloan, E. D.; Koh, C. A. *Clathrate Hydrates of Natural Gases*, 3rd ed.; CRC Press: Boca Raton, FL, 2008.
(4) Kelland, M. A. History of the development of low dosage hydrate inhibitors. *Energy Fuels* **2006**, *20*, 825−847.
(5) Kelland, M. A. A review of kinetic hydrate inhibitors: Tailormade water-soluble polymers for oil and gas industry applications. In *Advances in Materials Science Research*; Wytherst, M. C., Ed.; Nova Science Publishers, Inc: New York, 2011; Vol. *8*.
(6) Perrin, A.; Musa, O. M.; Steed, J. W. The chemistry of low dosage clathrate hydrate inhibitors. *Chem. Soc. Rev.* **2013**, *42*, 1996−2015.
(7) Zhukov, A. Y.; Stolov, M. A.; Varfolomeev, M. A. Use of Kinetic Inhibitors of Gas Hydrate Formation in Oil and Gas Production Processes: Current State and Prospects of Development. *Chem. Technol. Fuels Oils* **2017**, *53*, 377−381.
(8) Shahnazar, S.; Bagheri, S.; TermehYousefi, A.; Mehrmashhadi, J.; Abd Karim, M. S.; Kadri, N. A. Structure, mechanism, and performance evaluation of natural gas hydrate kinetic inhibitors. *Rev. Inorg. Chem.* **2018**, *38*, 1−19.
(9) Kamal, M. S.; Hussein, I. A.; Sultan, A. S.; von Solms, N. Application of various water soluble polymers in gas hydrate inhibition. *Renew. Sustain. Energy Rev.* **2016**, *60*, 206−225.
(10) Wang, Y.; Fan, S.; Lang, X. Reviews of gas hydrate inhibitors in gas-dominant pipelines and application of kinetic hydrate inhibitors in China. *Chin. J. Chem. Eng.* **2019**, *27*, 2118−2132.
(11) Makogon, T. Y. *Handbook of Multiphase Flow Assurance*; Elsevier Science & Technology, 2019.
(12) Chin, Y. D.; Srivastava, A.. In *Offshore Technology Conference*; : Houston, Texas, USA, 2018. 30 April - 3 May.*Advances in LDHIs and Applications, OTC-28905*
(13) Singh, A.; Suri, A. Review of Kinetic Hydrate Inhibitors Based on Cyclic Amides and Effect of Various Synergists. *Energy Fuels* **2021**, *35*, 15301−15338.
(14) Ivall, J.; Pasieka, J.; Posteraro, D.; Servio, P. Profiling the Concentration of the Kinetic Inhibitor Polyvinylpyrrolidone throughout the Methane Hydrate Formation Process. *Energy Fuels* **2015**, *29*, 2329−2335.
(15) Posteraro, D.; Ivall, J.; Maric, M.; Servio, P. New insights into the effect of polyvinylpyrrolidone (PVP) concentration on methane hydrate growth. 2. Liquid phase methane mole fraction. *Chem. Eng. Sci.* **2015**, *126*, 91−98.
(16) Lim, V. W. S.; Metaxas, P. J.; Johns, M. L.; Haandrikman, G.; Crosby, D.; Aman, Z. M.; May, E. F. The delay of gas hydrate formation by kinetic inhibitors. *Chem. Eng. J.* **2021**, *411*, 128478.
(17) Musa, O. M.; Lei, C. C. Polymers Having Acid and Amide Moieties, and Uses Thereof, U.S. Patent Application US 20,130,123,147 A1, 2013.
(18) Musa, O. M.; Lei, C. C. Polymers Having N-Vinyl Amide and Hydroxyl Moieties, Their Compositions and the Uses Thereof, U.S. Patent Application US 20,120,077,717 A1, 2012.
(19) Sheng, Q.; Silveira, K. C. d.; Tian, W.; Fong, C.; Maeda, N.; Gubner, R.; Wood, C. D. Simultaneous hydrate and corrosion inhibition with modified Poly(vinyl caprolactam) polymers. *Energy Fuels* **2017**, *31*, 6724−6731.
(20) Park, J.; Kim, H.; Sheng, Q.; Wood, C. D.; Seo, Y. Kinetic Hydrate Inhibition Performance of Poly(vinyl caprolactam) Modified with Corrosion Inhibitor Groups. *Energy Fuels* **2017**, *31*, 9363−9373.
(21) Pavelyev, R. S.; Zaripova, Y. F.; Yarkovoi, V. V.; Vinogradova, S. S.; Razhabov, S.; Khayarov, K. R.; Nazarychev, S. A.; Stoporev, A. S.; Mendgaziev, R. I.; Semenov, A. P.; Valiullin, L. R.; Varfolomeev, M. A.; Kelland, M. A. Performance of Waterborne Polyurethanes in Inhibition of Gas Hydrate Formation and Corrosion: Influence of Hydrophobic Fragments. *Molecules* **2020**, *25*, 5664.
(22) Farhadian, A.; Varfolomeev, M. A.; Rahimi, A.; Mendgaziev, R. I.; Semenov, A. P.; Stoporev, A. S.; Vinogradova, S. S.; Karwt, R.; Kelland, M. A. Gas Hydrate and Corrosion Inhibition Performance of the Newly Synthesized Polyurethanes: Potential Dual Function Inhibitors. *Energy Fuels* **2021**, *35*, 6113−6124.
(23) Ul-Haq, I.; Abdullah, A.; Al-Eid, M.; Al-Ajwad, H. A.; Acryloyl based polymers with active end cap as corrosion inhibitors, International Patent Application WO 2021119114 A1, 2021.
(24) Macedo, R. G. M. A.; Marques, N. D. N.; Tonholo, J.; Balaban, R. C. Water-soluble carboxymethylchitosan used as corrosion inhibitor for carbon steel in saline medium. *Carbohydr. Polym.* **2019**, *205*, 371−376.
(25) Bain, D. I.; Fan, G.; Fan, J.; Ross, R. J. Scale and Corrosion Inhibition by Thermal Polyaspartates. *Nace Corrosion Conference*, Paper 120, 1999.
(26) Fan, J. C.; Fan, L.-D. G.; Mazo, J. Composition and method for inhibition of metal corrosion, International Patent Application WO 2000075399 A3, 2000.
(27) Wang, C.; Chen, J.; Han, J.; Wang, C.; Hu, B. Enhanced corrosion inhibition performance of novel modified polyaspartic acid on carbon steel in HCl solution. *J. Alloys Compd.* **2019**, *771*, 736−746.
(28) Chen, J.; Wang, C.; Han, J.; Hu, B. S.; Wang, C. B.; Zhong, Y. L.; Xu, H. Corrosion inhibition performance of threonine-modified polyaspartic acid for carbon steel in simulated cooling water. *J. Appl. Polym. Sci.* **2019**, *136*, 47242.
(29) Chua, P. C.; Sæbø, M.; Lunde, A.; Kelland, M. A. Dual Kinetic Hydrate Inhibition and Scale Inhibition by Polyaspartamides. *Energy Fuels* **2011**, *25*, 5165−5172.
(30) Klug, P.; Kelland, M. Additives for inhibiting gas hydrate formation. US Patent Number 6,369,004 B1, 2002; https://patents.google.com/patent/US6369004B1/en.
(31) Zhang, Q.; Kelland, M. A. A new investigation of polymaleamides as kinetic hydrate inhibitors - Improved performance and compatibility with high salinity brines. *Chem. Eng. Sci.* **2021**, *241*, 116719.
(32) Kelland, M. A.; Pomicpic, J.; Ghosh, R.; Undheim, C.; Hemmingsen, T. H.; Zhang, Q.; Varfolomeev, M. A.; Pavelyev, R. S.; Vinogradova, S. S. Multi-functional oilfield production chemicals: maleic-based polymers for gas hydrate and corrosion inhibition. *IOP Conf. Ser. Mater. Sci. Eng.* **2021**, *1201*, 012081.
(33) Chua, P. C.; Kelland, M. A. Poly(N-vinyl azacyclooctanone): A More Powerful Structure II Kinetic Hydrate Inhibitor than Poly(N-vinyl caprolactam). *Energy Fuels* **2012**, *26*, 4481−4485.
(34) Myers, R. H.; Myers, S. L.; Walpole, R. E.; Ye, K. *Probability & Statistics for Engineers & Scientists*; Pearson Education Int.: New Jersey, U.S.A., 2007.
(35) Bannwarth, C.; Ehlert, S.; Grimme, S. GFN2-xTB-An Accurate and Broadly Parametrized Self-Consistent Tight-Binding Quantum Chemical Method with Multipole Electrostatics and Density-Dependent Dispersion Contributions. *J. Chem. Theory Comput.* **2019**, *15*, 1652−1671.
(36) Bannwarth, C.; Caldeweyher, E.; Ehlert, S.; Hansen, A.; Pracht, P.; Seibert, J.; Spicher, S.; Grimme, S. Extended Tight-Binding Quantum Chemistry Methods. *Wiley Interdiscip. Rev. Comput. Mol. Sci.* **2020**, *11*, No. e1493.
(37) Pracht, P.; Caldeweyher, E.; Ehlert, S.; Grimme, S. *A Robust Non-self-consistent Tight-Binding Quantum Chemistry Method for Large Molecules*; ChemRXIV, June 2019.
(38) Bursch, M.; Hansen, A.; Grimme, S. Fast and Reasonable Geometry Optimization of Lanthanoid Complexes with an Extended Tight Binding Quantum Chemical Method. *Inorg. Chem.* **2017**, *56*, 12485−12491.
(39) Struch, N.; Bannwarth, C.; Ronson, T. K.; Lorenz, Y.; Mienert, B.; Wagner, N.; Engeser, M.; Bill, E.; Puttreddy, R.; Rissanen, K.; Beck, J.; Grimme, S.; Nitschke, J. R.; Lützen, A. An Octanuclear Metallosupramolecular Cage Designed To Exhibit Spin-Crossover Behavior. *Angew. Chem.* **2017**, *56*, 4930−4935.
(40) Seibert, J.; Bannwarth, C.; Grimme, S. Biomolecular Structure Information from High-Speed Quantum Mechanical Electronic Spectra Calculation. *J. Am. Chem. Soc.* **2017**, *139*, 11682−11685.
(41) Pracht, P.; Bauer, C. A.; Grimme, S. Automated and efficient quantum chemical determination and energetic ranking of molecular protonation sites. *J. Comput. Chem.* **2017**, *38*, 2618−2631.
(42) Grimme, S. Exploration of Chemical Compound, Conformer, and Reaction Space with Meta-Dynamics Simulations Based on Tight-

https://doi.org/10.1021/acs.energyfuels.2c00075
Energy Fuels 2022, 36, 3088−3096

Binding Quantum Chemical Calculations. *J. Chem. Theory Comput.* **2019**, *15*, 2847−2862.
(43) Schmitz, S.; Seibert, J.; Ostermeir, K.; Hansen, A.; Göller, A. H.; Grimme, S. Quantum Chemical Calculation of Molecular and Periodic Peptide and Protein Structures. *J. Phys. Chem. B* **2020**, *124*, 3636−3646.
(44) Balcells, D.; Skjelstad, B. B. tmQM Dataset-Quantum Geometries and Properties of 86k Transition Metal Complexes. *J. Chem. Inf. Model.* **2020**, *60*, 6135−6146.
(45) Margraf, J. T.; Reuter, K. Pure non-local machine-learned density functional theory for electron correlation. *Nat. Commun.* **2021**, *12*, 344.
(46) Saha, I.; Dang, E. K.; Svatunek, D.; Houk, K. N.; Harran, P. G. Computational generation of an annotated gigalibrary of synthesizable, composite peptidic macrocycles. *Proc. Natl. Acad. Sci. U.S.A.* **2020**, *117*, 24679−24690.
(47) Schmitz, G.; Yönder, Ö.; Schnieder, B.; Schmid, R.; Hättig, C. An automatized workflow from molecular dynamic simulation to quantum chemical methods to identify elementary reactions and compute reaction constants. *J. Comput. Chem.* **2021**, *42*, 2264−2282.
(48) Serillon, D.; Bo, C.; Barril, X. Testing automatic methods to predict free binding energy of host-guest complexes in SAMPL7 challenge. *J. Comput. Aided Mol. Des.* **2021**, *35*, 209−222.
(49) Perdew, J. P.; Burke, K.; Ernzerhof, M. Generalized Gradient Approximation Made Simple. *Phys. Rev. Lett.* **1996**, *77*, 3865.
(50) Brandenburg, J. G.; Bannwarth, C.; Hansen, A.; Grimme, S. B97-3c: A Revised Low-Cost Variant of the B97-D Density Functional Method. *J. Chem. Phys.* **2018**, *148*, 064104.
(51) *Semiempirical Extended Tight-Binding Program Package Xtb*, Version 6.4.1; https://github.com/grimme-lab/xtb, 2021.
(52) Ehlert, S.; Stahn, M.; Spicher, S.; Grimme, S. Robust and Efficient Implicit Solvation Model for Fast Semiempirical Methods. *J. Chem. Theor. Comput.* **2021**, *17*, 4250−4261.
(53) Ferrero, R.; Pantaleone, S.; Delle Piane, M.; Caldera, F.; Corno, M.; Trotta, F.; Brunella, V. On the Interactions of Melatonin/*β*-Cyclodextrin Inclusion Complex: A Novel Approach Combining Efficient Semiempirical Extended Tight-Binding (xTB) Results with Ab Initio Methods. *Molecules* **2021**, *26*, 5881.
(54) Bannwarth, C.; Caldewehyer, E.; Hansen, A.; Pracht, P.; SeibertSpicher, S.; Grimme, S. Extended tight-binding quantum chemistry methods. *Wiley Interdiscip. Rev.: Comput. Mol. Sci.* **2021**, *11*, No. e1493.
(55) Hill, D. J. T.; O'Donnell, J. H.; O'Sullivan, P. W. Analysis of the mechanism of copolymerization of styrene and maleic anhydride. *Macromol* **1985**, *18*, 9−17.
(56) Fehérvári, F.; Azori, M.; Földes-Berezsnich, T.; Tudős, F. Analysis of the role of complex in the alternating copolymerization of N-vinylpyrrolidone and maleic anhydride. *Polym. Bull.* **1987**, *18*, 225−232.
(57) Veron, L.; Revol, M.; Mandrand, B.; Delair, T. Synthesis and characterization of poly(N-vinyl pyrrolidone-alt-maleic anhydride): Conjugation with bovine serum albumin. *J. Appl. Polym. Sci.* **2001**, *81*, 3327−3337.
(58) Popescu, I.; Prisacaru, A. I.; Suflet, D. M.; Fundueanu, G. Thermo- and pH-sensitivity of poly(N-vinylcaprolactam-co-maleic acid) in aqueous solution. *Polym. Bull.* **2014**, *71*, 2863−2880.
(59) Hu, G. H.; Lindt, J. T. Amidification of poly(styrene-co-maleic anhydride) with amines in tetrahydrofuran solution: A kinetic study. *Polym. Bull.* **1992**, *29*, 357−363.
(60) Ree, L. H. S.; Opsahl, E.; Kelland, M. A. N-Alkyl Methacrylamide Polymers as High Performing Kinetic Hydrate Inhibitors. *Energy Fuels* **2019**, *33*, 4190−4201.
(61) Cohen, J. M.; Wolf, P. F.; Young, W. D. Enhanced hydrate inhibitors: powerful synergism with glycol ethers. *Energy Fuels* **1998**, *12*, 216−218.
(62) Cohen, J. M.; Wolf, P. F.; Young, W. D. Method for preventing or retarding the formation of gas hydrates, U.S. Patent 5,723,524 A, 1998.
(63) Ree, L. H. S.; Kelland, M. A. Investigation of Solvent Synergists for Improved Kinetic Hydrate Inhibitor Performance of Poly(N-isopropyl methacrylamide). *Energy Fuels* **2019**, *33*, 8231−8240.
(64) Kelland, M. A.; Dirdal, E. G.; Ree, L. H. S. Solvent Synergists for Improved Kinetic Hydrate Inhibitor Performance of Poly(N-vinylcaprolactam). *Energy Fuels* **2020**, *34*, 1653−1663.
(65) Nakarit, C.; Kelland, M. A.; Liu, D.; Chen, E. Y.-X. Cationic kinetic hydrate inhibitors and the effect on performance of incorporating cationic monomers into N-vinyl lactam copolymers. *Chem. Eng. Sci.* **2013**, *102*, 424−431.
(66) Rebolledo-Libreros, M. E.; Reza, J.; Trejo, A.; Guzman-Lucero, D. J. Evaluation of copolymers from 1-vinyl-3-alkylimidazolium bromide and N-vinylcaprolactam as inhibitors of clathrate hydrate formation. *J. Nat. Gas Sci. Eng.* **2017**, *40*, 114−125.
(67) Klomp, U. C.; Kruka, V. C.; Reijnhart, R. A method for inhibiting the plugging of conduits by gas hydrates, International Patent Application WO 199517579 A1, 1995.
(68) Klomp, U. C.; Reijnhart, R. Method for inhibiting the plugging of conduits by gas hydrates, International Patent Application WO 199634177 A1, 1996.
(69) Chua, P. C.; Kelland, M. A. Tetra(iso-hexyl)ammonium Bromide-The Most Powerful Quaternary Ammonium-Based Tetrahydrofuran Crystal Growth Inhibitor and Synergist with Polyvinylcaprolactam Kinetic Gas Hydrate Inhibitor. *Energy Fuels* **2012**, *26*, 1160.
(70) Kelland, M. A.; Kvæstad, A. H.; Astad, E. L. Tetrahydrofuran Hydrate Crystal Growth Inhibition by Trialkylamine Oxides and Synergism with the Gas Kinetic Hydrate Inhibitor Poly(N-vinyl caprolactam). *Energy Fuels* **2012**, *26*, 4454−4464.
(71) Dirdal, E. G.; Kelland, M. A. Does the Cloud Point Temperature of a Polymer Correlate with Its Kinetic Hydrate Inhibitor Performance? *Energy Fuels* **2019**, *33*, 7127−7137.
(72) Lide, T.; Tandong, Y.; White, J. W. C.; Wusheng, Y.; Ninglian, W. Westerly Moisture Transport to the Middle of Himalayas Revealed from the High Deuterium Excess. *Chin. Sci. Bull.* **2005**, *50*, 1026−1030.
(73) Comuzzo, P.; Battistutta, F. Acidification and pH Control in Red Wines. In *Red wine technology*; Elsevier, 2019, pp 17−34. DOI: 10.1016/b978-0-12-814399-5.00002-5
(74) Popescu, I.; Prisacaru, A. I.; Suflet, D. M.; Fundueanu, G. Thermo- and pH-sensitivity of poly(N-vinylcaprolactam-co-maleic acid) in aqueous solution. *Polym. Bull.* **2014**, *71*, 2863−2880.
(75) Mansfield, K. F.; Theodorou, D. N. Molecular Dynamics Simulation of a Glassy Polymer Surface. *Macromolecules* **1991**, *24*, 6283−6294.
(76) Minagawa, K.; Matsuzawa, Y.; Yoshikawa, K.; Khokhlov, A. R.; Doi, M. Direct Observation of the Coil-Globule Transition in Dna Molecules. *Biopolymers* **1994**, *34*, 555−558.
(77) Deng, S.; Arinstein, A.; Zussman, E. Size-Dependent Mechanical Properties of Glassy Polymer Nanofibers via Molecular Dynamics Simulations. *J. Polym. Sci., Part B: Polym. Phys.* **2017**, *55*, 506−514.

https://doi.org/10.1021/acs.energyfuels.2c00075
Energy Fuels 2022, 36, 3088−3096